CrystEngComm

Accepted Manuscript

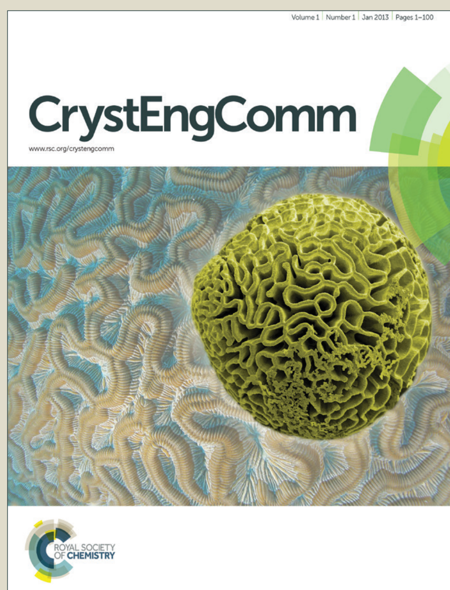

This is an *Accepted Manuscript*, which has been through the Royal Society of Chemistry peer review process and has been accepted for publication.

Accepted Manuscripts are published online shortly after acceptance, before technical editing, formatting and proof reading. Using this free service, authors can make their results available to the community, in citable form, before we publish the edited article. We will replace this *Accepted Manuscript* with the edited and formatted *Advance Article* as soon as it is available.

You can find more information about *Accepted Manuscripts* in the Information for Authors.

Please note that technical editing may introduce minor changes to the text and/or graphics, which may alter content. The journal's standard Terms & Conditions and the Ethical guidelines still apply. In no event shall the Royal Society of Chemistry be held responsible for any errors or omissions in this *Accepted Manuscript* or any consequences arising from the use of any information it contains.

ROYAL SOCIETY OF CHEMISTRY

www.rsc.org/crystengcomm

Experiments and analysis in the two-step growth of InGaAs on GaAs substrate

Jinping Li,[a] Guoqing Miao[*a] Zhiwei Zhang,[a] and Yugang Zeng,[*a]

[1]*State Key Laboratory of Luminescence and Applications, Changchun Institute of Optics, Fine Mechanics and Physics, Chinese Academy of Sciences, Changchun, 130033, China*

Abstract:

The two-step growth technique was introduced to solve the highly lattice-mismatched (5.6%) between $In_{0.78}Ga_{0.22}As$ and GaAs substrate, and the mechanisms of dislocation density reduction by the low-temperature buffer (LT-buffer) were investigated experimentally. In the case of different thickness of LT-buffer layers, the surface morphology and microstructure were investigated, and the residual strain and dislocation density of $In_{0.78}Ga_{0.22}As$ epitaxial layer were studied by XRD, Raman and the TEM, respectively. We proposed the mechanisms to explain the dislocation density reduction during the two-step growth process by the LT-buffer. Also the experimental results support our conclusion and verify the mechanism we presented.

[a] *State Key Laboratory of Luminescence and Applications, Changchun Institute of Optics, Fine Mechanics and Physics, Chinese Academy of Sciences, No.3888 Dongnanhu Road.* miaogq@ciomp.ac.cn, zengyg@ciomp.ac.cn.

CrystEngComm Accepted Manuscript

Introduction

The ternary Ⅲ-Ⅴ compound $In_xGa_{1-x}As$ with different In content has been extensively applied in fiber-optic communications and near-infrared photodetectors. To extend the response of detector to longer wavelength, the growth of $In_xGa_{1-x}As$ alloy with high In content (where $x > 0.53$) becomes necessary. Both InP and GaAs substrates have been used for the growth of $In_xGa_{1-x}As$, while the lattice-mismatch between them could lead to a deterioration of crystalline quality in epitaxial layer. Compared with $In_xGa_{1-x}As$/GaAs ($x > 0.53$), $In_xGa_{1-x}As$/InP ($x > 0.53$) has a smaller lattice-mismatch, but it suffers from several insuperable disadvantages including high fragility, immature process, etc.[1-4] Lower cost of GaAs as well as GaAs-based devices also has motivated the researchers to focus much attention on $In_xGa_{1-x}As$/GaAs system.

Lattice-mismatch gives rise to strain during the growth, which could degrade the crystalline quality of epitaxial layer. The buffer has been demonstrated to be effective to accommodate the lattice-mismatch. Composition linearly-graded and step-graded buffer layers were introduced to relieve the deterioration of $In_xGa_{1-x}As$ due to the lattice-mismatch.[5-11] The two-step growth technique has often been used in the growth of highly mismatched heterostructures in which epitaxial layers grown at high temperatures are followed by the low-temperature growth of buffer layers (namely LT-buffer). The employ of two-step growth in highly mismatched system (such as GaN/Al_2O_3,[12-13] GaN/SiC,[14] InSb/Si,[15] etc) brings a significant improvement in crystalline quality of epitaxial layers. In our previous works, two-step technique was demonstrated to be effective for the $In_{0.82}Ga_{0.18}As$/InP growth,[18-19] LT-buffer thickness and growth temperature of epitaxial layer were investigated experimentally, but without any studies concerning the models or mechanisms for LT-buffer.

CrystEngComm Accepted Manuscript

In the early years, Shou-Zen Chang [16] showed that the growth of the highly mismatched $In_xGa_{1-x}As/GaAs$ heterojunction favors the early relaxation of islands before they coalesce. Dislocation formation mechanism in strained $In_xGa_{1-x}As/GaAs$ was investigated by Y. Chen [17], the experimental results and analysis explained the changes from 60° dislocations to 90° dislocations at different lattice-mismatch. Although the LT-buffer layer is a crucial issue and it is important to understand the mechanisms that how the LT-buffer inhibits the deterioration of crystalline quality due to the lattice-mismatch, there has been few reports on the mechanisms.

In this paper, two-step growth was also used to grow $In_{0.78}Ga_{0.22}As/GaAs$ heterostructure, the LT-buffer was employed to prevent the dislocations propagating to the epitaxial layer and to relax the strain caused by lattice-mismatch. We studied the surface morphology of epitaxial layers. The residual strain and dislocation density in epitaxial layers were calculated, the results indicated that the LT-buffer is more effective at a certain thickness. Based on the experiments results and analysis, we proposed the mechanisms for dislocation density reduction by the LT-buffer.

CrystEngComm Accepted Manuscript

Experimental

All the samples discussed here were grown by MOCVD (AIXTRON 200/4) at low pressure (76 torr) with purified H_2 as carrier gas. Trimethylindium (TMIn), trimethylgallium (TMGa) and pure arsine (AsH_3) were used as the In, Ga and As precursors, respectively. The design of the sample was as follows: low-temperature buffer layer (LT-buffer) of InGaAs were grown on (001) GaAs substrates; the InGaAs LT-buffer was followed by the $In_{0.78}Ga_{0.22}As$ epitaxial layer. The growth conditions for five samples almost kept the same except the LT-buffer layer thickness: the LT-buffers of InGaAs were grown with a growth rate of 0.8 μm/h at 450℃ and $In_{0.78}Ga_{0.22}As$ epitaxial layers were grown with a growth rate of 1.4 μm/h at 650℃, the V/III ratio was 73 during the growth; Thickness of $In_{0.78}Ga_{0.22}As$ epitaxial layer was about 1 μm for all samples, and the InGaAs LT-buffer thickness studied here was 31nm, 85nm, 196nm and 269nm, which were determined by TEM, respectively.

High-resolution x-ray diffractometer (HRXRD, Bruker D8) was used for Omega-2Theta scan and Omega scan to investigate the crystalline quality of epitaxial layers. The surface morphology and roughness were examined by scanning electron microscope (SEM, Hitachi S4800) and atomic force microscopy (AFM, Bruker MultiMode 8). Raman spectrometer (RENISHAW InVia) was utilized to characterize the difference in the frequencies of the GaAs-like longitudinal optical (LO) phonons, which were used to calculate the residual strain in epitaxial layers. The dislocation density and structure properties of epitaxial layers were investigated by TEM (JEOL, JEM-2100F).

CrystEngComm Accepted Manuscript

Results and discussion

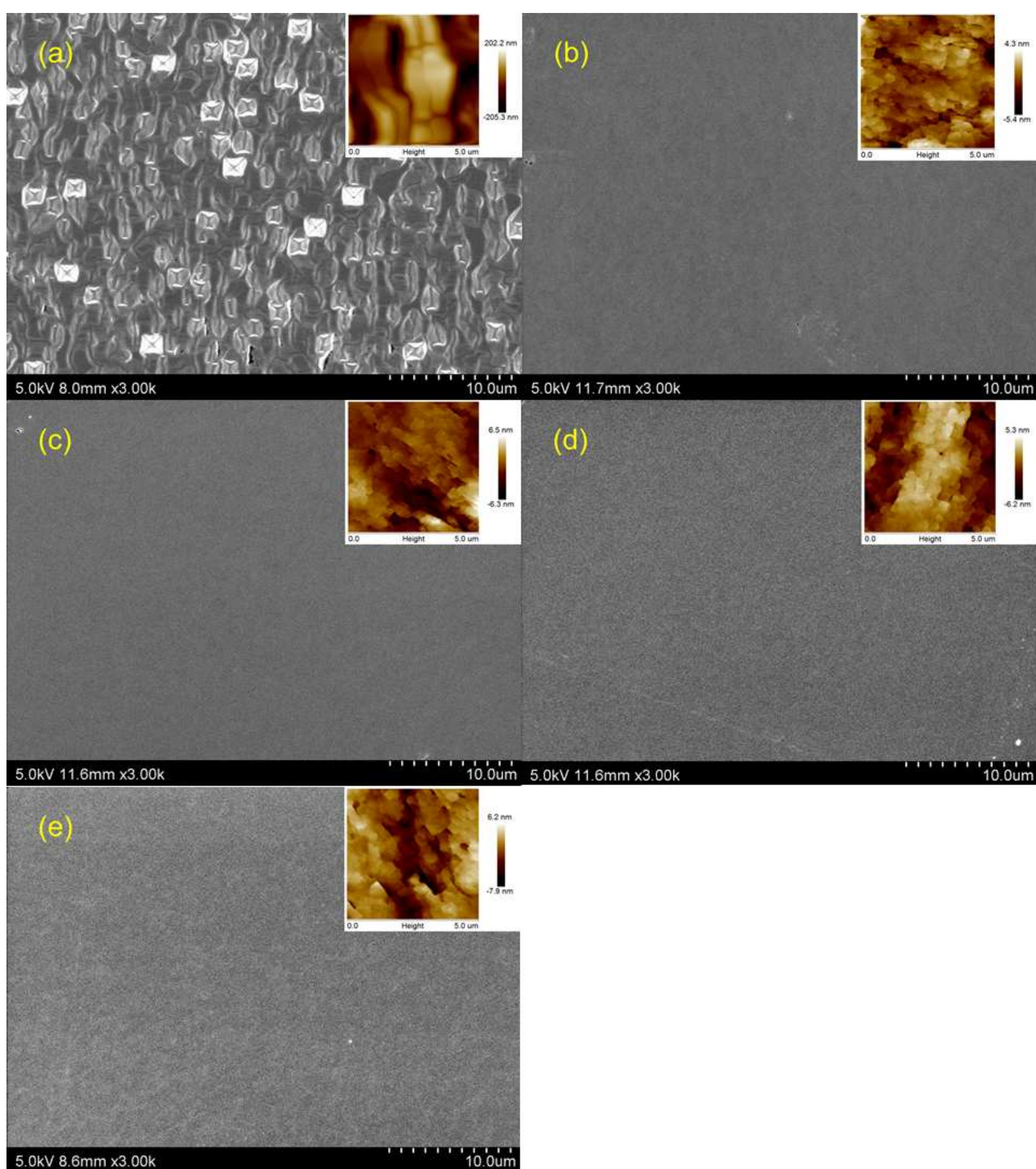

Fig.1. SEM and AFM images of $In_{0.78}Ga_{0.22}As$ epitaxial layers for sample A-E with different LT-buffer thickness: (a) 31nm, (b) 85nm, (c) 141nm, (d) 196nm and (e) 269nm, the corresponding AFM image is shown in insets.

CrystEngComm Accepted Manuscript

The surface morphology and roughness of $In_{0.78}Ga_{0.22}As$ epitaxial layer were examined by SEM and AFM. The LT-buffer thickness of five samples were 31nm, 85nm, 141nm, 196nm and 269nm, corresponding to sample A, B, C, D and E, respectively. Fig.1 (a)-(e) show SEM and AFM images of $In_{0.78}Ga_{0.22}As$ epitaxial layers grown with different thickness LT-buffer layers. Compared with the others, sample A with a 31nm LT-buffer layer (Fig.1. (a)) shows an irregular and rough surface, which is covered by pits and coalescence lines, exhibiting island growth and a poor surface. And sample B-E all exhibit a smooth and flat surface. Roughness of the five samples are summarized in Table. 1. Sample A possesses the poorest surface and the maximum roughness of 70.9nm. For sample B-E, the root mean square roughness of $In_{0.78}Ga_{0.22}As$ epitaxial layer increases from 1.21nm to 2.16nm with increasing the LT-buffer thickness, and sample B has the minimum roughness, which illustrates a best epitaxial layer surface of all.

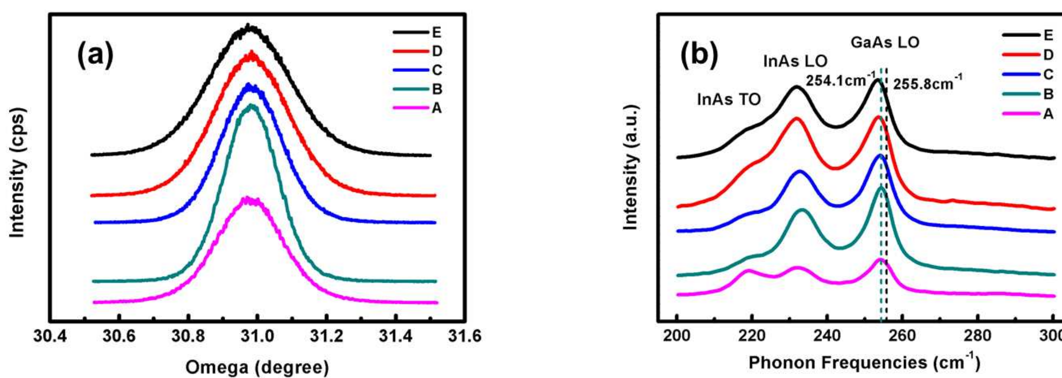

Fig.2. (a) Comparison between rocking curves of InGaAs epitaxial layer for sample A-E; (b) Raman spectra of InGaAs epitaxial layer for sample A-E.

CrystEngComm Accepted Manuscript

Table 1. Variation of roughness, full width at half maximum (FWHM), dislocation density (N_{dis} from rocking curves and ρ from TEM), frequency shift ($\Delta\omega_{LO}$) between ω_{LO} and ω_0, and strength of the residual strain (X) as a function of LT-buffer thickness.

Sample	Buffer thickness (nm)	Roughness (nm)	FWHM (degree)	N_{dis} (cm^{-2})	$\Delta\omega_{LO}$ (cm^{-1})	X (dyn*cm^{-2})	ρ (cm^{-2})
A	31	70.9	0.229	9.96E+8	1.84	-8.48E+10	3.46E+12
B	85	1.21	0.183	6.36E+8	1.69	-7.79E+10	1.06E+12
C	141	1.64	0.208	8.22E+8	1.76	-8.11E+10	1.48E+12
D	196	1.93	0.246	1.15E+9	2.12	-9.77E+10	2.87E+12
E	269	2.16	0.270	1.38E+9	2.83	-1.30E+11	3.07E+12

The full width at half maximum (FWHM) of $In_{0.78}Ga_{0.22}As$ epitaxial layers were obtained from the (004) x-ray rocking curves (RCs), which is shown in Fig. 2 (a). The FWHM values were summarized in Table 1. Except for sample A, FWHM of $In_{0.78}Ga_{0.22}As$ epitaxial layer increases along with the increase of LT-buffer thickness. The smallest FWHM of 0.183 degree was obtained in sample B, which provides the best crystalline quality compared to the others.

The dislocation density as a function of the FWHM of (004) RCs was estimated by the formula[20]

$$N_{dis} = (FWHM)^2 / 9b^2 \quad (1)$$

Where FWHM is in radians, b is the length of Burgers vector of dislocations. $b = a_0 / \sqrt{2}$ is used in all above cases where a_0 is the lattice constant of the epitaxial layer which was

CrystEngComm Accepted Manuscript

determined by Vegard's Law. Table. 1 lists the dislocation density of $In_{0.78}Ga_{0.22}As$ epitaxial layer in each sample. In terms of the above results, it can be concluded that the $In_{0.78}Ga_{0.22}As$ epitaxial layer of sample B with the smallest FWHM has the minimum dislocation density.

Strain relaxation has been investigated by means of Raman scattering in strained $In_{0.78}Ga_{0.22}As$ epitaxial layers under a (001) back-scattering geometry, and it is confirmed that the thickness (1μm) of $In_{0.78}Ga_{0.22}As$ epitaxial layers is far beyond the penetration depth.[21-22] By changing the In content, the lattice parameter of $In_xGa_{1-x}As$ alloy varies between GaAs and InAs ones. The GaAs and InAs bond lengths also change with the In content, so do the optical phonons frequencies.[23] In $In_xGa_{1-x}As$ alloys, the optical phonons exhibit both InAs- and GaAs-like modes over the whole composition range. The Raman spectra of $In_xGa_{1-x}As$ layers are observed somewhat differently by each author except for the highest band corresponding to the GaAs-like longitudinal optical (LO) mode.[24] Furthermore, the InAs-like mode sometimes is obscure[24] and the InAs-like LO frequencies remain almost constant when the In content changes.[23] Therefore, the GaAs-like LO mode will be employed to evaluate the residual strain in the $In_{0.78}Ga_{0.22}As$ epitaxial layers.[24]

Fig.2. (b) shows the (001) backscattering Raman spectra of epitaxial layers for different samples. Around 255cm^{-1} is the GaAs-like LO frequency, which is distinguishable for each case, and the InAs-like LO frequencies almost remain around 233cm^{-1}. In all samples, the InAs-like transverse optical (TO) frequency which should be forbidden in the configuration appears in the left shoulder of InAs-like LO frequency. According to Pearsall's study [25], the origin of InAs-like TO mode may be related to the crystalline disorder. And the nature of the misorientation still needs more investigations. Based the previous studies[26], the equation (2) was utilized to calculate the residual strain in $In_{0.78}Ga_{0.22}As$ epitaxial layer:

CrystEngComm Accepted Manuscript

$$X = \frac{3\omega_0 * \Delta\omega_{LO}}{(p+q)(S_{11}+2S_{12})-(p-q)(S_{11}-S_{12})} \quad (2)$$

$$\omega_0 = -32x^2 - 18.6x + 290.0 \quad (3)$$

Where X is the strength of the residual strain which is summarized in Table 1, x is the In content, p and q are the optical phonon deformation constants, S_{11} and S_{12} are the elastic compliance constants, ω_{LO} is the measured GaAs-like LO frequency in epitaxial layer, ω_0 is the GaAs-like LO frequency in the ideal strain-free bulk $In_xGa_{1-x}As$ alloy as a function of composition x, which could be obtained from the equation (3) reported by Shuichi Emura;[24] the residual strain in epitaxial layers is evaluated from the deviation $\Delta\omega_{LO}$ of the GaAs-like LO frequency, here $\Delta\omega_{LO}$ is the frequency shift between ω_{LO} and ω_0.

As shown in Fig.2. (b), the calculated GaAs-like LO frequency in the ideal strain-free bulk $In_{0.78}Ga_{0.22}As$ epitaxial layer is at 255.8cm^{-1}. Table 1 shows that the GaAs-like LO frequency of sample B has the minimum shifts with respect to 255.8cm^{-1}, and it is observed at 254.1cm^{-1}. The residual strain of $In_{0.78}Ga_{0.22}As$ epitaxial layer with different thickness LT-buffer was compared in Table 1. For sample B-E, the residual strain in epitaxial layers increases with the increase of LT-buffer thickness and sample B has the minimum residual strain value, which illustrates the best crystalline quality of all. For sample A, the buffer is too thin to accommodate the lattice-mismatch completely. Much strain introduced by lattice-mismatch was relaxed in epitaxial layer, as a consequence, although the epitaxial layer of sample A exhibits a poor crystalline quality, it has a small residual strain value. As can be seen from the results, the thicker LT-buffer is more effective within a certain thickness range and there should exist an optimal buffer thickness. Considering the crystalline quality of epitaxial layers declined with increasing LT-buffer

CrystEngComm Accepted Manuscript

thickness for sample B-E, we proposed that: In proportion as the LT-buffer thickness increase the energy induced by thermal strain will rise, more strain relaxation is needed in thicker LT-buffer layer than a thinner one. Therefore, the thicker LT-buffer layers would produce more dislocations, which might be propagated to the epitaxial layers. As a result, the crystalline quality of epitaxial layer deteriorated with the increase of LT-buffer thickness just as the residual strain values illustrated.

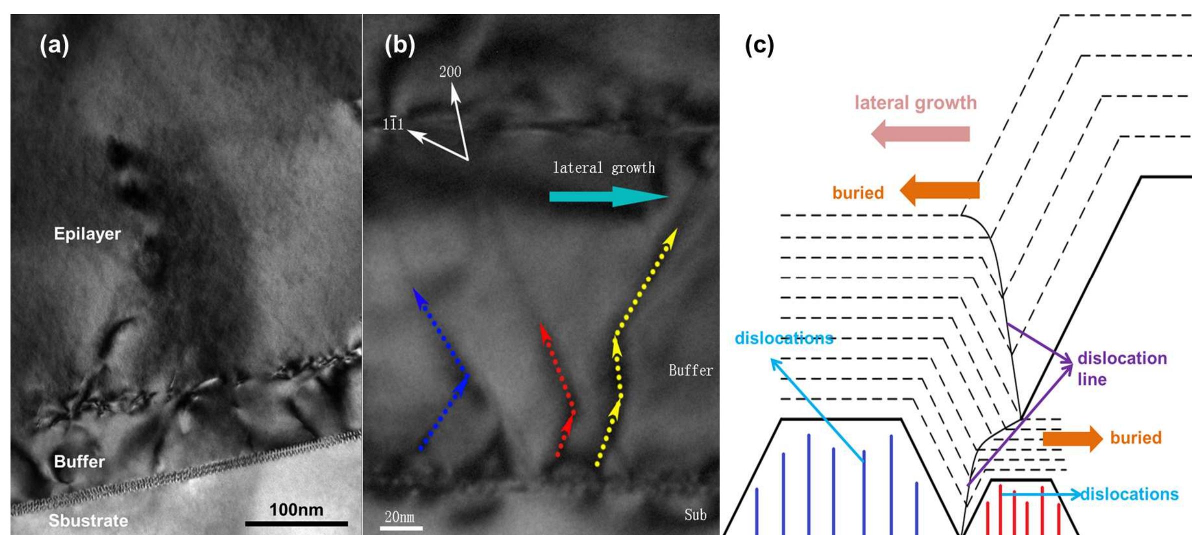

Fig.3. (a) Cross-sectional TEM micrograph of the $In_{0.78}Ga_{0.22}As$/LT-InGaAs/GaAs interface regions, (b) Dislocation bending in LT-buffer layer, (c) A brief schematic of LT-buffer layer grown on GaAs substrate

The transmission electron microscopy (TEM) was used to analyze the microstructure of the LT-buffer structure. Table. 1 shows the dislocation density (ρ) of $In_{0.78}Ga_{0.22}As$ epitaxial layer in different samples. We can conclude from the results that: sample A with the thinnest buffer has the maximum dislocation density, and sample B have the minimum dislocation density value. For sample B-E, the dislocation density increases with the LT-buffer thickness between 85nm and 269nm, and sample B has the best crystalline quality of epitaxial layer.

CrystEngComm Accepted Manuscript

The high-magnification cross-sectional TEM images (just like the Fig.3. (a) shows) were implemented to interpret the mechanisms for the dislocation density reduction by LT-buffer. There is a large (5.6%) lattice-mismatch and thermal expansion coefficient difference between LT-buffer layer and GaAs substrate. Therefore, the LT-buffer layer showed an island growth, and numerous islands with different size were generated as growth. Driven by the lateral growth, numerous islands were buried. These islands contained numerous dislocations, leading to an effective strain relaxation.

A brief model was established in Fig.3. (c): after the initial formation of the islands, the lateral growth drives them to coalesce. For the islands with different size, once the bottom of the slightly larger islands touch the neighboring small islands, the larger islands would bury the small islands on account of the lateral growth rate difference between them, resulting in the crooked dislocation lines (labeled by the dotted line in Fig.3. (b)). However, when the buffer thickness is thin, which means that the growth plane has not been covered by the islands yet or the buffer layer has just shaped, the islands will be hardly buried. In following growth, the larger islands bury the small islands continuously and the dislocation lines are bent back and forth, as a result, numerous dislocations located in the small islands will be blocked down. As the continuous growth of LT-buffer, the size of islands becomes larger and the islands become similar in size to each other, resulting in a quantity reduction of buried islands. For instance, the blue dotted line in Fig.3. (b) shows that: Initially, the dislocation line inclines to the right, blocking the right neighboring small island, after a short distance of propagation along the original direction, the dislocation line is bent to left when the former island is confronted with a larger island which has a faster lateral growth rate. Then, the left island is buried by the right island as well as the dislocations located in the islands.

CrystEngComm Accepted Manuscript

The results from the XRD, Raman and TEM all illustrate that: the buffer is too thin or too thick will lead to a poor crystalline quality of $In_{0.78}Ga_{0.22}As$ epitaxial layer. Based on the analysis above, we proposed that: when the LT-buffer is too thin, there is not much coalescence between islands, which means most islands contain dislocations will not be buried, then, the dislocations are propagated into epitaxial layer, leading to a deteriorated crystalline quality. If the LT-buffer is too thick, the size difference between islands will become smaller, and this reduces the quantity of the buried islands, then, the unblocked dislocations would be propagated into epitaxial layer. This explains the changing trend of dislocation density in epitaxial layers for sample B-E by TEM, and confirms the buried islands model to some extent. Furthermore, in proportion as the LT-buffer thickness increase the energy induced by thermal strain will rise, and this in turn increases the dislocation density in LT-buffer layer. The quantity of the dislocation increase caused by thermal strain is larger than the dislocation reduction by the buried islands, hence, more dislocations in LT-buffer layer will be propagated into epitaxial layer.

CrystEngComm Accepted Manuscript

Conclusion

In summary, the two-step growth method was adopted to grow the $In_{0.72}Ga_{0.28}As/GaAs$ structures with different LT-buffer thickness. We investigated the surface morphology and microstructure by XRD, AFM, Raman and TEM. The results showed that: For the high In content InGaAs/GaAs system, two-step growth was effective for relieving the crystalline quality deterioration of epitaxial layer due to the large lattice-mismatch. We found that there exists an appropriate thickness of LT-buffer to make it work more effectively. And we proposed the mechanisms for dislocation density reduction: the LT-buffer layer displays an island growth mode during the two-step growth, since the lateral growth rate and size of islands differ from each other, numerous islands contain dislocations are buried during the coalescences, suppressing the propagation of dislocations as growth. The experimental results support our conclusion and verify the mechanisms we proposed. It's anticipated that our work will play an important role in the design of buffer layer and dislocation analysis under the large lattice-mismatch system in the future.

Acknowledgements

This work was supported by the National Key Basic Research Program of China (Grant No. 2012CB619201).

CrystEngComm Accepted Manuscript

Notes and references

1. K. R. Linga, A. M. Joshi, V. S. Ban, and S. M. Mason, *SPIE's 1993 International Symposium on Optics, Imaging, and Instrumentation. International Society for Optics and Photonics*, 1993, **2021**, 90.
2. L. Zhou, Y. G. Zhang, X, Y Chen, Y. Gu, H. S. B. Y. Li, Y. Y. Cao, and S. P. Xi, *Journal of Physics D: Applied Physics*, 2014, **47**, 085107.
3. G. R. Lin, H. C. Kuo, C. K. Lin, and M. Feng, *IEEE Journal of Quantum Electronics*, 2005, **41**, 749.
4. A. Ren, X. M. Ren, Q. Wang, D. Xiong, H. Huang, and Y. Q. Huang, *Microelectronics journal*, 2006, **37**, 700.
5. M. D. Scott, A. H. Moore, A. J. Moseley, A.J. Moseley, and R.H. Wallis, *Journal of Crystalline Growth*, 1986, **77**, 606.
6. Y. G. Zhang, Y. Gu, Z. B. Tian, A. Z. Li, X. G. Zhu, and Y. L. Zheng, *Infrared Physics & Technology*, 2008, **51**, 316.
7. A. Gocalinska, M. Manganaro, and E. Pelucchi, *Applied Physics Letters*, 2012, **100**, 152112.
8. Y. Gu, Y.G. Zhang, K. Wang, X. Fang, C. Li, L. Zhou, A.Z. Li, and Hsby. Li, *Journal of Crystalline Growth*, 2013, **378**, 65.
9. G. H. Olsen, A.M. Joshi, S.M. Mason, K.M. Woodruff, E. Mykietyn, V.S. Ban, M.J. Lange, J. Hladky, G.C. Erickson and G.A. Gasparian, *33rd Annual Techincal Symposium. International Society for Optics and Photonics*, 1990, 276.
10. A. Krier, D.Chubb, SE. Krier, M.Hopkinson, G.Hill, Optoelectronics, *IEE Proceedings-. IET*, 1998, **145**, 292.
11. M.A. di Forte-Poisson, C. Brylinski, Di Persio J, J. di Persio, X. Hugon, B. Vilotitch and C.

CrystEngComm Accepted Manuscript

Le Noble, *Journal of crystalline growth*, 1992, **124**, 791.

12. S. Nakamura, Y. Harada, M. Seno, *Applied physics letters*, 1991, **58(18)**, 2021.
13. S. Nakamura, *Japanese Journal of Applied Physics*, 1991, **30(10A)**, L1705.
14. P. Waltereit, C. Poblenz, S. Rajan, F. Wu, U. K. Mishra and J. S. Speck, *Japanese journal of applied physics*, 2004, **43(12A)**, L1520.
15. Y. H. Kim, J. Y. Lee, Y. G. Noh, M. D. Kim, Y. J. Kwon, J. E. Oh and R. Gronsky, *Applied physics letters*, 2006, **89(3)**, 031919.
16. S. Z. Chang, T. C. Chang and S. C. Lee, *Journal of applied physics*, 1993, **73**, 4916.
17. Y. Chen, X. W. Lin, Z. LilientalWeber, J. Washburn, J. F. Klem, and J. Y. Tsao, *Applied physics letters*, 1996, **68,** 111.
18. T. Zhang, G. Miao, Y. Jin, S. Yu, H. Jiang, Z. Li and H. Song, *Materials Science in Semiconductor Processing*, 2009, **12(4)**, 156.
19. T. Zhang, G. Miao, Y. Jin, S. Yu, H. Jiang, Z. Li and H. Song, *Journal of alloys and compounds*, 2009, **472(1)**, 587.
20. S. Z. Chang, T. C. Chang, J. L. Shen, S. C. Lee, and Y. F. Chen, *Journal of applied physics*, 1993, **74**, 6912.
21. J. P. Estrera, P. D. Stevens, R. Glosser, W. M. Duncan, Y. C. Kao, H. Y. Liu and E. A. Beam III, *Applied physics letters*, 1992, **61(16)**, 1927.
22. G. Abstreiter, E. Bauser, A. Fischer and K. Ploog, *Applied physics*, 1978, **16(4)**, 345.
23. J. Groenen, G. Landa, R. Carles, P. S. Pizani, and M. Gendry, *Journal of applied physics*, 1997, **82**, 803.
24. E. Shuichi, G. Shun-ichi, M. Yaichi and H. Hideki, *Physical Review B*, 1988, **38**, 3280.
25. T. P. Pearsall, R. Carles and J. C. Portal, *Applied Physics Letters*, 1983, **42(5)**, 436.

CrystEngComm Accepted Manuscript

26. B. Jusserand, P. Voisin, M. Voos, L. L. Chang, E. E. Mendez, and L. Esaki, *Applied Physics Letters*, 1985, **46,** 678.

CrystEngComm Accepted Manuscript

Figures and tables

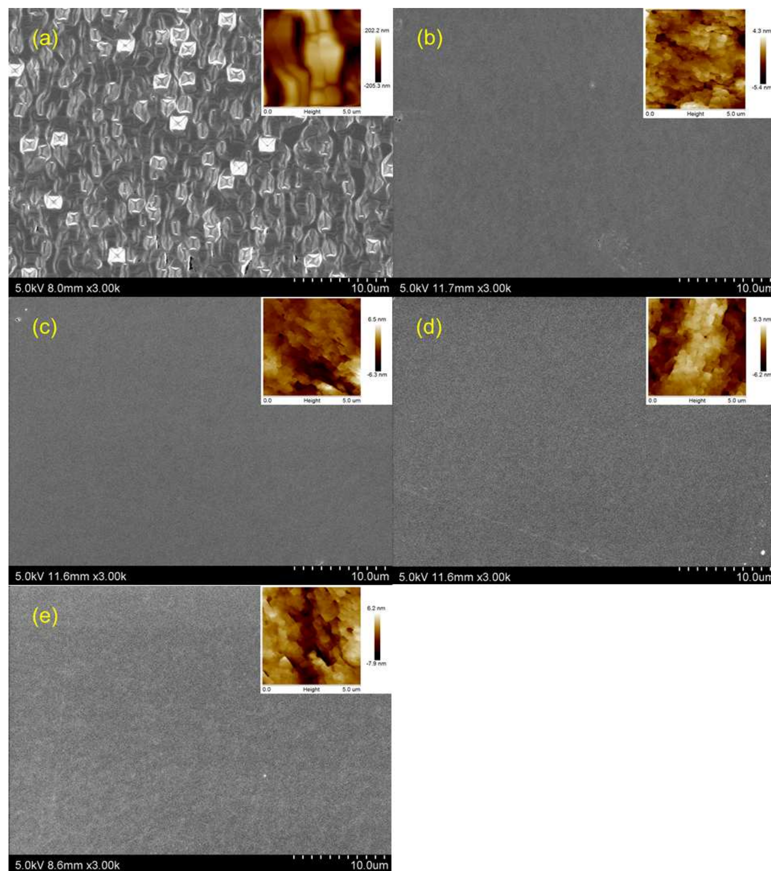

Fig. 1

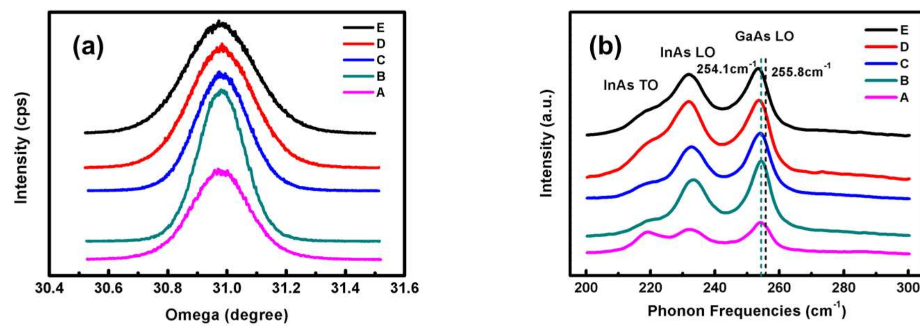

Fig. 2

CrystEngComm Accepted Manuscript

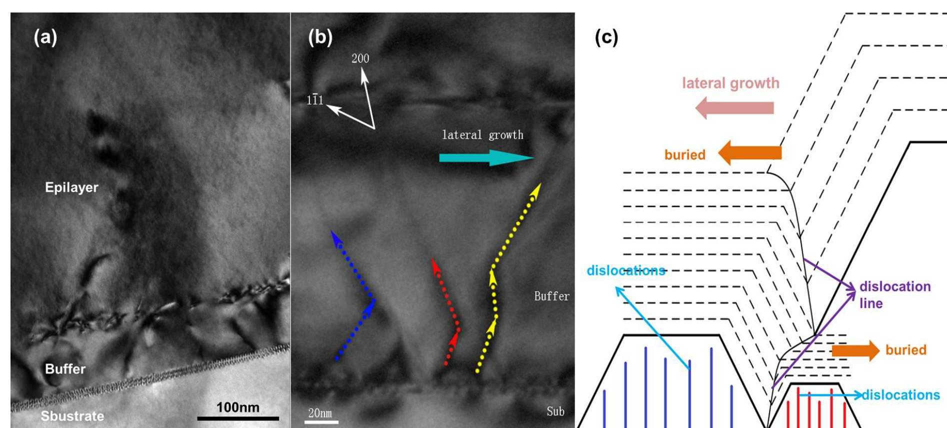

Fig. 3

Table. 1

Sample	Buffer thickness (nm)	Roughness (nm)	FWHM (degree)	N_{dis} (cm^{-2})	$\Delta\omega_{LO}$ (cm^{-1})	X ($dyn*cm^{-2}$)	ρ (cm^{-2})
A	31	70.9	0.229	9.96E+8	1.84	-8.48E+10	3.46E+12
B	85	1.21	0.183	6.36E+8	1.69	-7.79E+10	1.06E+12
C	141	1.64	0.208	8.22E+8	1.76	-8.11E+10	1.48E+12
D	196	1.93	0.246	1.15E+9	2.12	-9.77E+10	2.87E+12
E	269	2.16	0.270	1.38E+9	2.83	-1.30E+11	3.07E+12

CrystEngComm Accepted Manuscript

Figure and Table Captions

Fig. 1. SEM and AFM images of $In_{0.78}Ga_{0.22}As$ epitaxial layers for sample A-E with different LT-buffer thickness: (a) 31nm, (b) 85nm, (c) 141nm, (d) 196nm and (e) 269nm, the corresponding AFM image is shown in insets.

Fig. 2. (a) Comparison between rocking curves of InGaAs epitaxial layer for sample A-E; (b) Raman spectra of InGaAs epitaxial layer for sample A-E.

Fig. 3. (a) Cross-sectional TEM micrograph of the $In_{0.78}Ga_{0.22}As$/LT-InGaAs/GaAs interface regions, (b) Dislocation bending in LT-buffer layer, (c) A brief schematic of LT-buffer layer grown on GaAs substrate

Table. 1. Variation of roughness, full width at half maximum (FWHM), dislocation density (N_{dis} from rocking curves and ρ from TEM), frequency shift between ω_{LO} and ω_0 ($\Delta\omega_{LO}$), and strength of the residual strain (X) as a function of LT-buffer thickness.

CrystEngComm Accepted Manuscript

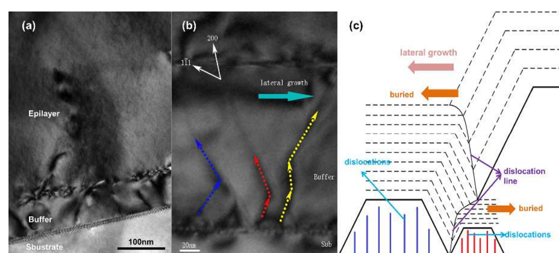

In this work, the mechanisms have been proposed to explain the dislocation density reduction in epitaxial layer by the LT-buffer.

CrystEngComm Accepted Manuscript